

# Reservoir Simulation Study for CO<sub>2</sub> Sequestration in Saline Aquifers

Chawarwan Khan

Lei Ge

Victor Rudolph

School of Chemical Engineering  
University of Queensland  
Australia

## Abstract

*Sequestration of carbon dioxide in geological formations has been recognised as one of the most promising ways to cope with greenhouse gas emissions, and saline aquifers are one of the potential storage target. This study evaluates feasibility of CO<sub>2</sub> storage in saline aquifers under different conditions. Simulation studies are carried out based on a homogeneous aquifer model. Compositional reservoir simulator (CMG-GEM) was used to simulate 10 years of CO<sub>2</sub> injection phase and simulate the fate of CO<sub>2</sub> post injection from hundreds to thousands of years. Different subsets of sensitive parameters are independently investigated to understand the impact of various parameter son different trapping mechanisms. Simulation results are also compared with other published research studies to provide additional insight of factors affecting CO<sub>2</sub> sequestration process.*

**Keywords:** CO<sub>2</sub> injection, solubility trapping, residual trapping, mineral trapping

## 1. Introduction

### 1.1 Theory Background

The permanent sequestration of CO<sub>2</sub> captured from power stations and industrial sources is one of the major options for reducing greenhouse gas emissions. Injection into petroleum reservoirs is widely considered the most promising method, since it is an established practice for enhancing oil recovery, and the storage site is well characterised and known to be secure against gas leakage (Condor et al. 2010). The process has provided confidence that long term storage is possible in appropriate selected geological storage reservoirs (Benson 2006). Another candidate system for CO<sub>2</sub> injection is into saline aquifers. These have the advantages of having very large capacity, are broadly distributed and most importantly they underlie most CO<sub>2</sub> emission sources (Hitchon et al. 1996). Estimates of worldwide sequestration capacity is large, with saline aquifers having he biggest potential capacity, followed by oil and gas reservoirs and then coal bed methane reservoirs (IPCC 2005). Furthermore, CO<sub>2</sub> is a promising candidate for geo-sequestration since it has high solubility in water and a high density as a supercritical fluid at reasonable depths (>800m) where pressures are relatively high (Bachu and Adams 2003; Bachu 2008).

### 1.2 Storage Mechanisms

CO<sub>2</sub> injection into aquifers for sequestration purposes is trapped through different mechanisms namely, structural, residual, solubility and mineral trapping (IPCC 2005; Bachu 2003). These processes may be tracked through numerical models that have been developed to predict the extent of each trapping mechanism under different conditions of interest (Prevost et al. 2005). In almost all cases the CO<sub>2</sub> would be injected as a supercritical fluid (scCO<sub>2</sub>). As injection of CO<sub>2</sub> proceeds, at the start, the CO<sub>2</sub> saturates the interstitial space in the zone around the well as it displaces brine. Generally, the CO<sub>2</sub> injection is into the lowest layers of reservoir, since this provides a number of advantages, mainly more effective brine ‘drainage’ (through buoyant displacement). The scCO<sub>2</sub> density is much less than the brine, so it rises under buoyancy until a geological seal layer is reached (Bachu 2008). The CO<sub>2</sub> pools under the seal layer and is retained by way of the structure trapping mechanism (Bachu et al. 2007). In addition, some dissolution of CO<sub>2</sub> occurs into formation water whenever the phases are in contact. This CO<sub>2</sub> is stored through the solubility trapping mechanism (Bachu et al. 1994).

As CO<sub>2</sub> dissolves into the brine according to local pressure, temperature and salinity conditions (Nghiem et al. 2004), the brine density increases, and the CO<sub>2</sub> heavy saturated brine moves downwards under gravity, causing some mixing and potentially exposing additional unsaturated brine to scCO<sub>2</sub>. This enhances solubility trapping and changes the extent of the CO<sub>2</sub> plume. The higher density fluids re-imbibe into the lower parts of the scCO<sub>2</sub> plume where there are layers of higher permeability trapping and immobilising CO<sub>2</sub> pockets within a continuous brine (liquid) phase (Bachu 2008; Juanes et al. 2006). This CO<sub>2</sub> is trapped under the residual mechanism, an important process when considering the long term fate of the CO<sub>2</sub> (Bachu et al. 2007). Some dissolved CO<sub>2</sub> dissociates into bicarbonate in the aqueous brine and these react species present in the fluid and rock resulting in dissolution and precipitation of different minerals (Gunter et al. 1993). These geo-chemical reactions of CO<sub>2</sub>\_Brine\_Rock result in carbonate precipitates, designated mineral trapping (Bachu and Adams 2003). The mineral trapping reactions may be very slow, even hundreds of years, but is considered to be the safest mechanism for CO<sub>2</sub> storage because of the stability of the precipitates. The scCO<sub>2</sub> directly under the cap rock probably remains as fluid pool in the reservoir and due to its buoyancy seeks to rise, where opportunity presents. This poses a risk of leakage of this fluid depending on the cap rock properties of the reservoir. In a suitable sequestration site, cap rock should have very low permeability and very high water retention by capillarity. Even so, it may be expected that a fraction of the CO<sub>2</sub> will diffuse into the cap rock (Bildstein 2010). The security of the storage depends entirely on the integrity of the seal over long period of time (Kumar et al. 2005), including that there are no natural fractures fissures or high permeability gaps in the cap.

### 1.3 Literature Review of Relevant Simulation Studies

Simulation of CO<sub>2</sub> geo-sequestration into saline reservoirs, has received considerable research attention and there are a variety of studies reported in the literature, examining different aspects and perspective. In general, while there may be some differences in detail (e.g., different reservoir characteristics, rock or/and fluid models) the outcomes are broadly consistent. This section presents a brief summary of some of the published studies that cover topics related to the objectives of this study. These also provide a basis for comparing the case studies conducted here to provide insights regarding CO<sub>2</sub> injection and long term geological storage. Ghanbari et al. (2006) simulated an example aquifer for CO<sub>2</sub> injection. The objective of the study was to investigate key parameters that affect the solubility trapping mechanism, in particular the effect of convective flow patterns. The study concluded which cases potentially maximise solubility trapping and also noted that the buoyancy drive caused by density differences enhances the CO<sub>2</sub> dissolution process. Ukaegbu et al. (2009) also presents an aquifer simulation model for CO<sub>2</sub> injection. The study examined effects of different parameters on CO<sub>2</sub> storage and the hysteresis effect on solubility trapping mechanisms. The primary focus of this study was to illustrate the distribution of CO<sub>2</sub> between the gaseous and aqueous phases under different aquifer conditions. The results suggested that hysteresis effects decrease CO<sub>2</sub> dissolution. Heterogeneity is important in simulation models, since permeability changes lateral migration behaviour of the CO<sub>2</sub> plume, especially where shales or mudstones layers create baffles above the layers where CO<sub>2</sub> is injected.

Both simulation studies (Ghanbari et al. 2006) and (Ukaegbu et al. 2009) used the generalized equation-of-state model-greenhouse gas (GEM-GHG) software package from Computer Modelling Group (CMG). Neither attempted to simulate mineral trapping Nghiem et al. (2004) describe a fully coupled geochemical process for simulating CO<sub>2</sub> sequestration in saline aquifers also using GEM-CMG. The primary objective of their study focused on mineral dissolution and precipitation kinetics. The study also considered convection of high density plumes of brine saturated with CO<sub>2</sub> and CO<sub>2</sub> mineralisation in the formation around the plumes. Nghiem et al. (2004) showed that CO<sub>2</sub> trapped by mineral trapping is less than soluble trapping at early stage of evaluation and mineralisation takes thousands of years to be fully realised. Pruess et al. (2003) simulated aquifer disposal of CO<sub>2</sub> using the TOUGHREACT simulator. The study investigated both mineral and solubility trapping mechanisms, and illuminated porosity and permeability changes that occur during trapping processes. The results suggested that under favourable conditions the amount of CO<sub>2</sub> that could be sequestered by mineralisation is comparable and can even be bigger to the amount of CO<sub>2</sub> that could be dissolved and held through solubility trapping. This conclusion was supported in a study conducted by (Xu et al. 2003). The studies of (Pruess et al. 2003) and (Xu et al. 2003) did not consider the effects of buoyancy as pointed out by (Ghanbari et al. 2006). Izgec et al. (2008) used CMG-STARS, a compositional and thermal reservoir simulator to model an aquifer for CO<sub>2</sub> injection coupled with geochemical changes. The results suggested that the CO<sub>2</sub> solubility trapping is larger than mineral trapping.

Law et al. (1995) simulated carbonate Nisku and Glauconitic sandstone aquifers by using the CMG-STARs simulator. The objective of their study was to investigate the capacity of these two aquifers to accept large quantities of CO<sub>2</sub> and retain the injected CO<sub>2</sub> for long periods of time. Since their study mainly was investigating injectivity, residual and mineral trapping mechanisms were ignored. Ide et al. (2007) simulated an aquifer to investigate residual trapping (including hysteresis effects) using the Eclipse simulator. The results indicated that significant amounts of the injected CO<sub>2</sub> will be trapped and that this trapping mechanism operates relatively quickly. In addition, the authors illustrated that aquifer inclination leads to enhance residual trapping mechanism. Flett et al. (2007) compared homogeneous and heterogeneous aquifer effects on residual trapping using the CHEARS black oil simulator. The reported results from this study showed that an increase in heterogeneity could delay residual trapping of CO<sub>2</sub>, as plume migration through such formations might be severely inhibited. Flett et al. (2007) also stated that the impact of heterogeneity needs be considered in CO<sub>2</sub> storage modelling for more accurate results and this applies also to the formation seal., Hovorka et al. (2004) using TOUGH2 simulator on a heterogeneous sandstone aquifer (Frio Framtion/Texas) supported this conclusion by stating the heterogeneity dominates the CO<sub>2</sub> plume behaviour since its migration is overwhelmingly permeability dependant.

Mo and Akervoll (2005) simulated geo-sequestration in an aquifer using Eclipse for both solubility and residual trapping mechanisms. The simulation results suggested that solubility trapping dominates CO<sub>2</sub> storage. In addition, Mo and Akervoll (2005) noted that an increase in anisotropy permeability ratio ( $K_v/K_h$ ) leads to a decrease in the amount of CO<sub>2</sub> trapped by residual trapping. Doughty (2006) conducted simulation studies to investigate residual trapping by using TOUGH2. He concluded that a hysteresis model should be used for aquifer simulations, since it more accurately captures the behaviour of the CO<sub>2</sub> plume and potentially also provides support for applications in geological settings where structural traps are absent or uncertain. Ozah et al. (2005) used the GEM-GHG simulator to study the sensitivity of CO<sub>2</sub> storage by considering three trapping mechanisms (residual, solubility and mineral trapping). The study concluded that the amount of CO<sub>2</sub> sequestered by mineral trapping is smaller than the other mechanisms, even over long timescales. In addition, horizontal wells could be effective in minimising gas loss from the aquifer and benefit trapping. Kumar et al. (2005) studied CO<sub>2</sub> storage in deep saline aquifers using GEM-CMG for three tapping mechanisms. They suggested that residual gas saturation contributes an important role in solubility trapping. Further, under some circumstances CO<sub>2</sub> storage by residual trapping (hysteresis included) can be larger than that due to solubility and mineral trapping. Pruess and Xu (2007) used TOUGHREACT to investigate residual gas saturation effects on CO<sub>2</sub> dissolution. The result accorded with the study by Kumar et al. (2005). In addition,

Audigane et al. (2007) reported that Ennis-King et al., (2002) investigated effects of residual water saturation on CO<sub>2</sub> dissolution, and concluded that solubility trapping was more important than the residual gas. Nghiem et al. (2010) also investigated the relationship between solubility and residual trapping based on various isotropic horizontal and vertical permeability values. The results suggested that these two mechanisms are competing storage processes (Nghiem et al. 2010). For example, increase in CO<sub>2</sub> storage under residual trapping leads to have less CO<sub>2</sub> available in the formation as a free phase and result in CO<sub>2</sub> solubility reduction. Kumar and Bryan (2008) conducted simulation studies particularly to investigate the plume behaviour and CO<sub>2</sub> trapping under different injection strategies. They reported that, for horizontal wells, residual trapping occurs along the well length direction. With a horizontally elongated plume which migrates vertically. This arrangement reduces trapping in lateral direction, unless the well length is very long. Sifuentes et al, 2009 simulated aquifers using ECLIPSE to assess the factors contributing to uncertainty during CO<sub>2</sub> injection and storage. They show that dissolution trapping is dominated by horizontal permeability and that residual trapping is affected by the controls on residual gas saturation. Juanes et al. (2006) simulated a saline aquifer for CO<sub>2</sub> injection using ECLIPSE. The purpose of the study was investigating the impact of relative permeability hysteresis on CO<sub>2</sub> storage. The simulation results suggested that accounting for hysteresis effects is necessary since it attempts to reduce CO<sub>2</sub> migration and accumulated CO<sub>2</sub> along the seal layer.

## **2. Aquifer Model Development**

### **2.1 Simulation of Geological Model**

The GEM simulation package Computer Modelling Group (CMG-GEM 2012) is used here for the simulation. The built in grid building module “Builder” generates the geological model of the reservoir, in this case a simple three-dimensional Cartesian geometry.

A limited size (9000 grid blocks) though not descriptive of any ‘real’ reservoir, is sufficient for our purpose which is to provide insight into the sensitivities of the different trapping mechanisms to changes in the system inputs which are varied individually and systematically. The grid has 30 blocks in the ‘I’ direction, 30 blocks in ‘J’ direction and 10 blocks in ‘K’ “vertical” direction, making up the 9000 grid blocks. The size of the blocks is arbitrary, but is assigned length and width of 70 m each, and 30m vertically. The fluid flow comprises two fluid phases, namely CO<sub>2</sub> and saline water. The reservoir is isothermal at 45 °C. The depth of the top layer of the reservoir is taken to be 1265 m with the pressure of 12400 kPaG which keeps CO<sub>2</sub> condition as supercritical (Table 1).

**Table 1: Aquifer Properties for the Initial Condition**

Aquifer Property	Value
Reservoir depth	1265 m
Aquifer Thickness (z direction)	300 m (10×30)
Width “m”	1050 m (30×70)
Length “m”	1050
Rock Compressibility	$4.5 \times 10^{-7} \text{ kPa}^{-1}$
Initial reservoir temperature	45 °C
Initial reservoir pressure	12400 kPa
Diffusion coefficient for CO <sub>2</sub>	0.000028 cm <sup>2</sup> /s
Salinity	10000 ppm
Dip angle	0 degrees

### 2.1.1 Rock Property

For the rock, the properties e.g., absolute permeability, effective porosity and water-gas relative permeability (Table2 and Figure1), are taken from experimental measurements on Berea sandstone (Evans 2012). The water-scCO<sub>2</sub> relative permeability curves used in the simulation are shown as graphs in Figure 1. The end point of water relative permeability curve is 1.0 at a residual scCO<sub>2</sub> saturation of zero; the end point for scCO<sub>2</sub> relative permeability curve is 0.16 at an irreducible water saturation of 0.45.

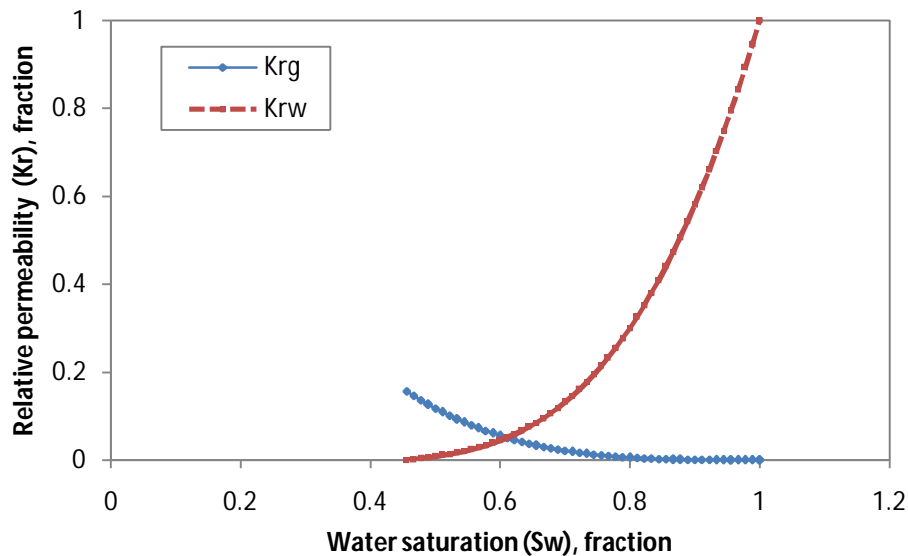


**Figure 1: Brine and Gas Relative Permeability for the Base Case**

**Table 2: Characteristics of the Core Sample Used for the Property Determination**

Sample ID	Lithology	Length, cm	Diameter, cm	Porosity, %	Permeability, mD
Berea, B2	Sandstone	7.98	3.79	21	165

### 2.1.2 Fluid Property

CMG-WinProp provides the phase behaviour and the properties of reservoir fluids (CMG-WinProp 2012). The formation is initially saturated with brine which includes a minimal trace of methane ( $C_1$ ) to facilitate convergence or computational stability (Ukaegbu et al., (2009); Ofori and Engler 2011; CMG-WinProp 2012). Under Winprop-GHG, For the  $CO_2$ -Brine- $C_1$  mixture the pure component  $C_1$  and  $CO_2$  properties and sc $CO_2$  phase density are estimated using Peng-Robinson Equation of State (Peng and Robinson 1976).  $CO_2$  solubility is modelled with Henry's law (Li and Nghiem 1986) for brine at a salinity of 10000 ppm. The brine phase viscosity and density are estimated by using Rowe and Chou (1970) correlation and Kestin et al. (1981) correlation, respectively. The sc $CO_2$  viscosity is predicted from the Jossi, Stiel and Thodos correlation (Reid et al. 1977).

### 2.1.3 Well Recurrent

A single injector in the middle of the aquifer is used and completed in the bottom layers (layers 8, 9 and 10). The injection well works under two constraints: the primary constraint is a maximum injection rate of ( $89200 \text{ m}^3/\text{day}$ ) at standard condition (SC); the secondary constraint is maximum bottom-hole pressure ( $28300 \text{ kPa -g}$ ), (Table 3).

**Table 3: Parameters of the Injection well**

Grids well completion (I, J; K)	15, 15, 8-10
Injection duration	10 years
Well radius	0.0762 m
Skin	0
$CO_2$ mole fraction	1
Maximum Bottom-hole Pressure	28300 kPag
Maximum injection rate (SC)	$89200 \text{ m}^3/\text{day}$

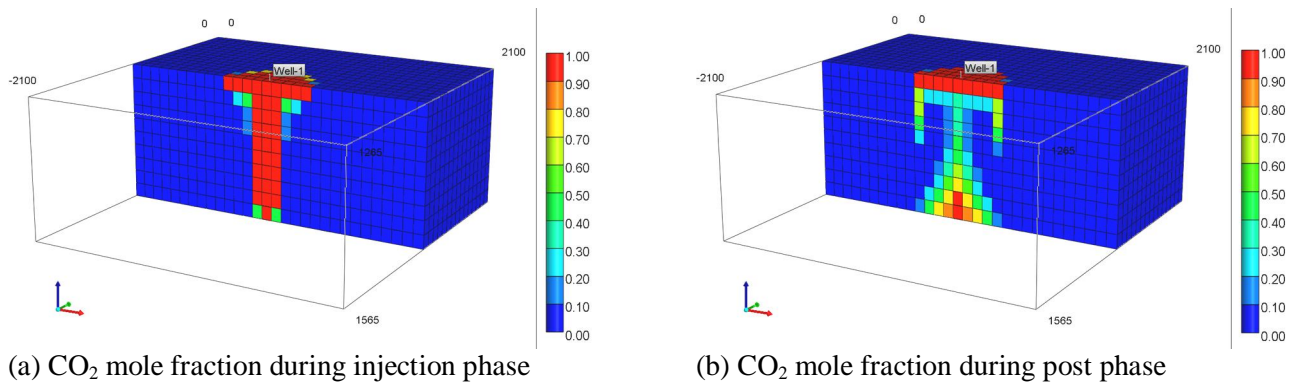
## 3. Simulation Strategy

The numerical simulation model is developed in two main categories, (1) hydrodynamic cases which correspond to structural, residual and dissolution trapping mechanisms, (2) geo-chemical cases, which correspond to the mineral trapping and coupled with the hydrodynamic trapping mechanisms. Different variables are then systematically altered to determine the effect of the parameter on various trapping mechanisms. The parameters are changed one at a time with the others held constant to isolate the different effects, although this loses interactions if two or more changes are made simultaneously.

### 3.1 Hydrodynamic Case Studies

#### 3.1.1 Base Case

The base case (Table 1, 2 and 3) against which the comparisons are made uses a single, centrally located sc $CO_2$  injection well. Injection occurs at a constant rate over 10 years, and the  $CO_2$  fate then modelled for a further 190 years, The residual fluid properties for the base case are taken as: 45% residual irreducible brine (where sc $CO_2$  is the continuous fluid phase, the brine retained in the formation as disconnected drops); 0% residual  $CO_2$  (where brine flood back into the formation, displacing sc $CO_2$  and re-establishing as the continuous phase) (Figure 1). The latter implies that the sc $CO_2$  in zones experiencing imbibition is either displaced (becomes part of the structurally trapped component) or is dissolved in the brine (becomes part of the solubility trapped  $CO_2$ ). Since for  $CO_2$  geo-storage, structural trapping is the highest risk (least secure) category, this represents a 'worst case' scenario – minimum, namely zero, residual  $CO_2$  trapping. The model permits the plume development to be followed over the whole period and the individual cells to be interrogated for their average properties: for example Figure 2 shows the degree of  $CO_2$  dissolved in the brine in each cell For the base case, after 200 years the distribution of the  $CO_2$  is: 67.2% as free sc $CO_2$  (structurally trapped); 32.8% dissolved in brine within the volume impacted by the plume (trapped by other mechanisms, here lumped as solubility trapped). Figure 2 and the following the 3D figures represent as the reservoir cross sectional incut through the middle (in the J direction), which is the grid block that contains the injector well.

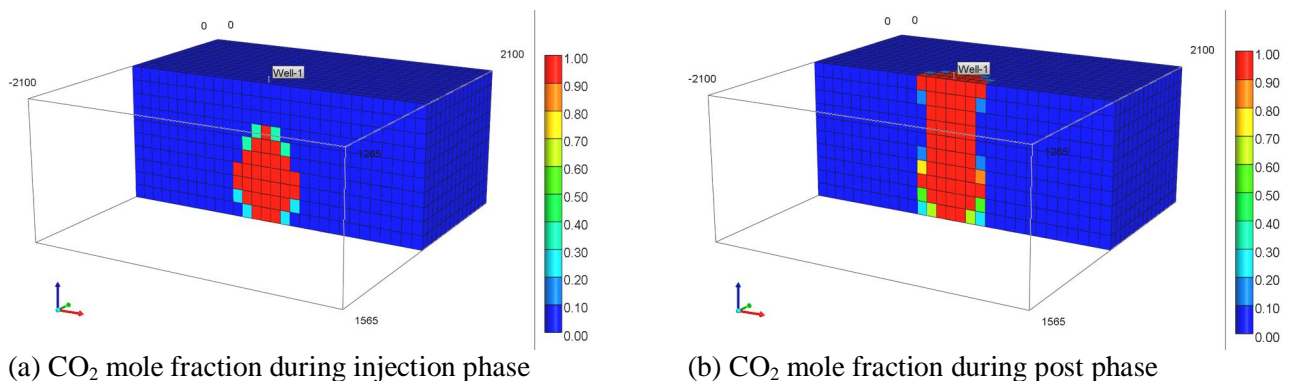
(a) CO<sub>2</sub> mole fraction during injection phase(b) CO<sub>2</sub> mole fraction during post phase**Figure 2: Base-Case Profiles Showing CO<sub>2</sub> Mole Fraction in Aqueous Phase**

### 3.1.2 Effect of Changing System Properties

Injection is controlled at a constant rate, so the total quantity of CO<sub>2</sub> placed into the reservoir is the same for all the cases examined. What changes is the extent to which each trapping mechanism contributes to the CO<sub>2</sub> storage. This is important because structural trapping is less secure than solubility trapping in regards to long term storage security.

**Horizontal permeability effects:** For higher horizontal permeability (illustrated here using  $K_h = 350$  mD) the plume spreads out more readily and contacts a larger volume of brine, resulting in more solution trapping (an increase of ~6% over the base case). The result is in agreement with the findings of Kumar et al. (2005) and Ofori and Engler (2011).

**Vertical to Horizontal Permeability Ratio ( $K_v/K_h$ ) effects:** The same base-case aquifer was simulated, however lower vertical permeability was considered ( $K_v$  of 10 md) in order to allow a better comparison. The simulation results indicated that decrease in  $K_v$  decreases the rate of vertical migration of gas during injection period. Under this case, a more lateral movement of the injected CO<sub>2</sub> is observed and forming an egg-shaped, almost around the depletion area (Figure 3).

(a) CO<sub>2</sub> mole fraction during injection phase(b) CO<sub>2</sub> mole fraction during post phase**Figure 3: Figure:  $K_v/K_h$ -Case Profiles Showing CO<sub>2</sub> Mole Fraction in Aqueous Phase**

After cessation of injection, CO<sub>2</sub> concentration starts to rise upward and results in enhanced CO<sub>2</sub> solubility. Kumar et al. (2005) and Ofori and Engler (2011) showed similar effects of  $K_v/K_h$  ratio on CO<sub>2</sub> solubility and propagation. In this case, the total dissolved CO<sub>2</sub> in the brine is increased by 7.071% compared to the base case dissolution.

**Porosity effects:** Porosity affect the space that is available for holding CO<sub>2</sub> in the sc-phase, and the quantity of brine that is available for solubilisation. When porosity is reduced (0.15 vs 0.21 in the base case) the dissolved CO<sub>2</sub> in the brine is lower initially, but at the very late stages slightly overtakes the base case, illustrating the competitive effects of less available brine per unit volume of reservoir vs wider dispersion of the plume, i.e., impacting a greater overall volume. This result agrees with the study conducted by (David 1996).

**Diffusivity effects:** The base-case was simulated without considering diffusion factor. CO<sub>2</sub> dissolution under both cases was same from beginning of the evaluation (first 25 years). Then, the dissolution of CO<sub>2</sub> remained lower for the rest of the simulation period.

Overall, the dissolved  $\text{CO}_2$  in the formation is decreased by 0.621% compared to the base case at the end of post injection. That is, the dissolved  $\text{CO}_2$  induce  $\text{CO}_2$  concentration gradients and causes  $\text{CO}_2$  to diffuse within the aquifer and observing more  $\text{CO}_2$  concentration in the grid blocks. Similarly, a simulation study was performed by Ghanbari et al. (2006) and the result was consistent with this case study.

**Salinity effects:** Under a case where higher salinity (250,000 ppm) is considered, the base case was used to predict  $\text{CO}_2$  solubility in the aquifer and illustrate  $\text{CO}_2$  profiles during and after injection process. The results showed that higher salt loads lead to increase the density of the brine, which increases plume buoyancy and causes the sc $\text{CO}_2$  phase to rise more quickly; and it reduces the solubility of  $\text{CO}_2$  in the water phase (Alkan et al. 2010; Ofori and Engler 2011). The end result is a significant increase in structural trapping below the seal (a high risk trap) and a reduction in solubility trapping (a low risk mechanism). Accordingly, the dissolved  $\text{CO}_2$  in the brine is less than the base case by 20.21% at the end of post injection.

**Temperature effects:** The same mechanisms apply as for salinity, lower temperature increases the density of the water phase and reduces the solubility of the  $\text{CO}_2$  in it. A 10C reduction in reservoir temperature compared to the base case reduces the solubility trapped  $\text{CO}_2$  by about 1%.

**Dip effects:** Reservoirs and seal caps are seldom perfectly horizontal. A dip angle of  $30^\circ$  serves to demonstrate the effect that this has on  $\text{CO}_2$  distribution, a significant increase in  $\text{CO}_2$  dissolution (~16% above the base case). In addition, the plume trapped below the seal rises under buoyancy up dip, spreading the plume in the lateral direction. This potentially provides a chance for  $\text{CO}_2$  to find its path through fissures cap rock and escape. Also, the brine saturated with  $\text{CO}_2$  migrates downwards, to the deeper edges of the reservoir during the convection process (Figure 4). These observations are in agreement with results obtained by (Sifuentes et al. 2009).

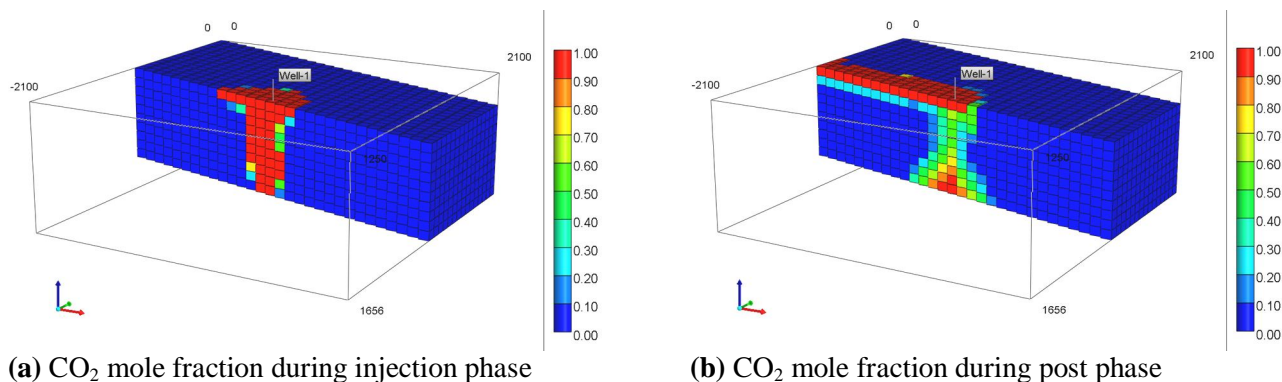


**Figure 4: Figure: Dip-Case Profiles Showing  $\text{CO}_2$  Mole Fraction in Aqueous Phase**

**Injection well completion interval effects:** The way that the injection well is completed affects the position of injection, the fluid fluxes near the injection point in the reservoir and consequently the plume shape. In the base case the injector was completed in the last two layers (bottom 60 m) of the 300 m thick reservoir. This is compared with the case where the bottom 3 layers (90m) are completed. Increasing injection well completion interval may allow faster  $\text{CO}_2$  injection, so that the bottom hole injection pressure reaches the maximum limit faster (David1996; Ghanbari et al. 2006). However, in the cases simulated here, the injection rate and the bottom-hole pressure, in either case, never reaches the maximum limit. The results indicate that, while during injection slightly more  $\text{CO}_2$  is dissolved in the brine for the 90m completion interval than for 60m, because the greater injection interval provides a larger contact volume, at the end of the simulation period, the 60m interval allows (slightly) more  $\text{CO}_2$  to be stored in solubility trapping. A useful summary of base case scenario for  $\text{CO}_2$  solubility trapping mechanism under different conditions is given in Table 4.

**Table 4: Summary of the Simulation Results for CO<sub>2</sub> Solubility under Different Conditions**

Simulation Scenarios	Fraction dissolved	
	injection phase	(post injection)
Base case	0.20	0.33
Horizontal perm increased from 165 mD to 350mD	0.20	0.39
Kv changed from 165to 10	0.20	0.40
Porosity reduced from 0.21 to 0.15	0.17	0.33
Diffusivity	0.20	0.32
Salinity increased from 10,000 to 250,000 ppm	0.10	0.13
Temperature changed from 45C to 35C	0.20	0.32
Dip angle changed from 00 to 30	0.21	0.49
Well-completion (from 2 layers 60m to 3 layers, 90m)	0.18	0.33

**Residual trapping mechanisms:** Since the base case, scCO<sub>2</sub> displaces the water phase as it is injected, but even in the zones where CO<sub>2</sub> is the continuous phase, residual water remains as droplets or wet zones surrounded by scCO<sub>2</sub>. The residual water is taken to be 45% of the rock voids. After injection is complete, as a result of density differences, the CO<sub>2</sub> migrates upward, and brine flows back into the areas of the formation that have previously been invaded by CO<sub>2</sub> (Bachu 2008). In the base case and cases considered so far, it has been assumed that this water could completely displace the scCO<sub>2</sub> (e.g., no residual gas saturation Fig 6), but in practice it is more the case that some residual scCO<sub>2</sub> remains behind as droplets or small pockets. This so-called residual CO<sub>2</sub> trapping is examined here. The starting point of gas saturation modified from zero to 0.022. The purpose of the modification was to simulated residual trapped gas saturation. In addition, this scenario is also investigated by considering hysteresis effect. The classical Land’s model (Land, 1968) is used to estimate hysteresis trapped gas saturation (Figure 5). The purpose of this study is to investigate the effects of these two trapping scenarios on the total residual trapping mechanisms.

$$S_{gt}^* = \frac{S_{gi}^*}{1 + CS_{gi}^*} \dots\dots\dots (1)$$

$$C = \frac{1}{S_{gt,max}} - \frac{1}{S_{g,max}} \dots\dots\dots (2)$$

S<sub>g, max</sub>: is the maximum gas saturation (0.55)

S<sub>gt, max</sub>: is the maximum trapped gas saturation (0.4).

The simulation results suggested that residual and solubility trapping mechanisms are playing two opposite forces during the storage processes. Table 5, increase in CO<sub>2</sub> storage under residual trapping lead to decrease CO<sub>2</sub> storage under solubility trapping mechanisms. The reason behind this phenomenon is that, residual trapping mechanism reduces the contact between injected CO<sub>2</sub> and brine in the aquifer. This will lead to provide less CO<sub>2</sub> available in the reservoir to migrate upward and in turn causes reduction in CO<sub>2</sub> concentration in the areas along the seal. The amount of CO<sub>2</sub> retained due to hysteresis effect is eventually exposed to the brine formation more horizontally than vertically and this leads to reduction in residual trapping and increase in CO<sub>2</sub>dissolution (Nghiem et al. 2009; Nghiem et al. 2010). This observation confirms that hysteresis is favourable for the effectiveness of CO<sub>2</sub> sequestration and potentially reduces risk of leakage. Since, total residual trapping mechanism plays an important part in predicting CO<sub>2</sub> storage. Therefore, this case is selected to investigate and illustrate CO<sub>2</sub> under mineral trapping mechanism and effects of dissolution and precipitation processes on the rock properties (e.g., permeability and porosity).

**Table 5: Hysteresis Effects on Solubility and Residual Trapping Mechanisms**

Trapping Mechanism Types	Residual Trapping through 0.022 Sgr without Hysteresis		Residual Trapping (Sgr 0.022) with Hysteresis	
	Injection phase	Post injection	Injection phase	Post injection
Free CO <sub>2</sub> Phase	0.754	0.631	0.642	0.511
Total Residual Trapping	0.060	0.041	0.215	0.264
Solubility Trapping	0.186	0.328	0.143	0.226

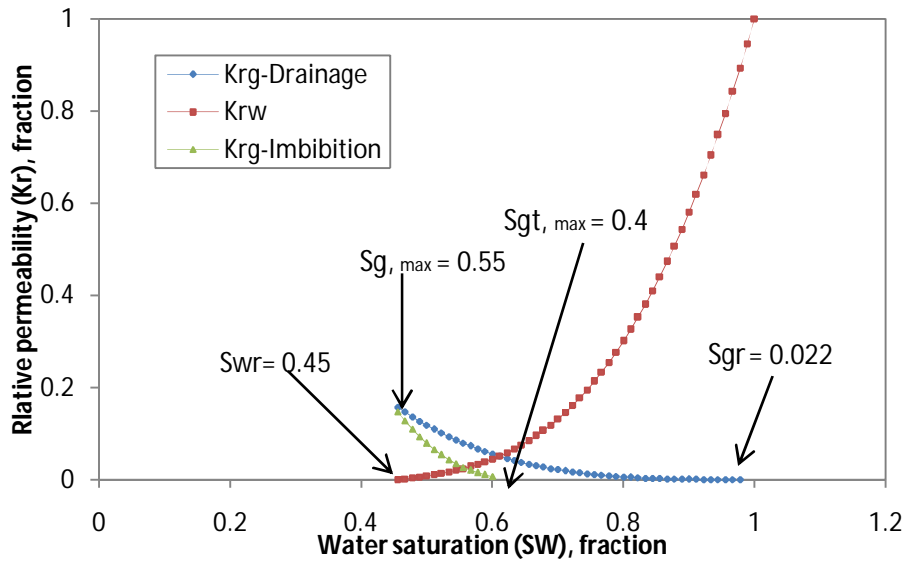


**Figure 5: Brine and Gas Relative Permeability Included Residual and Hysteresis Gas Saturation**

**3.1.3 Geo-Chemical Case Study**

One of the ultimate mechanisms for geo-sequestration of CO<sub>2</sub> is by mineralisation. The extent of this mineral trapping mechanism depends on the chemistry of formation water and rock mineralogy (Gunter et al. 1993). Dissolution and precipitation of carbonate solids are modelled here using the base-case properties, along with residual phase and hysteresis effects ( $S_{gr}=0.022$  and  $S_{gt,max} = 0.4$ , (Figure 7)) as an additional trapping mechanism, as one ultimate store of the injected CO<sub>2</sub>. Since many of the chemical reactions are slow (IPCC, 2005), it is necessary to consider timeframes much longer than for the other trapping mechanisms, here extended to 1000 years. For the present purposes the formation is assumed to be composed of 6 minerals dominated by Siderite and Annite, with water compositions shown in Table 6, and the initial mineral compositions in Table 7. The parameters used for modelling the mineral precipitation/dissolution rate reactions are shown in Table 8. The reaction equations for the minerals present in the aquifer rock are shown in Table9 (Total et al. 2007; Nghiem et al. 2010; Nghiem et al. 2011).

**Table 6: Initial Concentration of the Aqueous Species in the Aquifer**

Aqueous Species	Concentration Mole/kg H <sub>2</sub> O
H+	2.1925E-7
Al+++	2.4316E-14
Ca++	1.1049E-02
Mg++	1.9939E-02
SiO2(aq)	3.0097E-04
K+	5.8463E-03
Fe++	2.4842E-5
OH-	2.1201E-07
HCO3-	3.7571E-3
CO3--	3.9274E-6
AlOH++	1.5072E-12

**Table 7: Properties and Initial Volume Fraction of the Minerals**

Mineral Names	Mineral formulas	Molecular Weight g/mol	Density kg/m <sup>3</sup>	Initial volume fraction
Calcite	CaCO <sub>3</sub>	100	2709.95	0.0088
Dolomite	CaMg(CO <sub>3</sub> ) <sub>2</sub>	184.4034	2864.96	0.0088
Siderite	FeCO <sub>3</sub>	115.8562	4046.67	0.4968
Koalinite	Al <sub>2</sub> Si <sub>2</sub> O <sub>5</sub> (OH) <sub>4</sub>	258.1603	2594.05	0.0176
Illite	Mg <sub>0.25</sub> K <sub>0.6</sub> Al <sub>2.3</sub> Si <sub>3.5</sub> O <sub>12</sub> H <sub>2</sub>	383.9006	2763.07	0.0264
Quartz	SiO <sub>2</sub>	60.0843	2648.29	0.0088
Annite	ALKFe <sub>3</sub> Si <sub>3</sub> O <sub>10</sub> (OH) <sub>2</sub>	511.8859	3317.47	0.044
Anorthite	CaAL <sub>2</sub> Si <sub>2</sub> O <sub>8</sub>	278	2760.29	0.0088

**Table 8: kinetic Rate Parameters for Minerals Considered in the Simulation**

Mineral	Rate Constant Log <sub>10</sub> K <sub>β</sub> mol/m <sup>2</sup> .s	Reactive Surface Area A <sub>β</sub> m <sup>2</sup> /m <sup>3</sup>	Activation Energy E <sub>aβ</sub> J/mole
Calcite	-8.78	88	41870
Koalinite	-13	17600	62760
Illite	-14	26400	58620
Quartz	-13.9	7128	87500
Dolomite	-9.22185	88	41870
Annite	-14	4400	58620
Anorthite	-12	88	67830
Siderite	-9.22	88	41870

**Table 9: Geochemical Reaction**

Intra-aqueous chemical equilibrium reactions	
1	$CO_{2(aq)} + H_2O = H^+ + HCO_3^-$
2	$CO_3^{2-} + H^+ = HCO_3^-$
3	$OH^- + H^+ = H_2O$
4	$ALOH^{++} + H^+ = AL^{+++} + H_2O$
Mineral dissolution/precipitation reactions	
5	$Calcite + H^+ = Ca^{2+} + HCO_3^-$
6	$Dolomite + 2H^+ = Ca^{++} + Mg^{++} + 2HCO_3^-$
7	$Siderite + H^+ = HCO_3^-$
8	$Kaolinite + 6H^+ = 5H_2O + 2SiO_2(aq) + 2Al^{3+}$
9	$Illite + 8H^+ = 5H_2O + 0.6K^+ + 0.25Mg^{++} + 2.3AL^{+++} + 3.5SiO_2(aq)$
10	$(aq) Quartz = SiO_2(aq)$
11	$Annite + 10H^+ = 3Fe^{++} + K^+ + Al^{+++} + 3.5SiO_2(aq) + 6H_2O$
12	$Anorthite = 8H^+ = Ca^{++} + 2Al^{+++} + 2SiO_2(aq) + 4H_2O$

**Mineral trapping mechanism:** From the beginning of injection, areas around the well are saturated with the injected CO<sub>2</sub> (e.g., as a free phase) through displacing brine away from the wellbore as a function of given permeability. Dissolution of CO<sub>2</sub> within water formation occurs through mass transfer from CO<sub>2</sub> phase to aqueous phase whenever the two phases are in contact. Figure 6, shows the evolution of the total moles of CO<sub>2</sub> in terms scCO<sub>2</sub> rich phase (g), and in aqueous phase as dissolved CO<sub>2</sub> (aq) and as HCO<sub>3</sub><sup>-</sup> (Gunter et al. 1993). The dissolved CO<sub>2</sub> dissociates into ions proton H<sup>+</sup> and bicarbonate HCO<sub>3</sub><sup>-</sup>.

The process of CO<sub>2</sub> solubility continues as long there is free CO<sub>2</sub> phase and results in increasing HCO<sup>3-</sup>. As a result, the proton will result in acid solutions and the possibility of attack on the initial minerals present in the formation (David 1996). Accordingly, the minerals (except quartz) start to dissolve as long there is enough H<sup>+</sup> and generate ions (e.g., Ca<sup>++</sup> from Anorthite and Calcite, Mg<sup>++</sup> from Illite, Fe<sup>++</sup> from Annite) in the system. Then, the generated ions from the mineral dissolution process are combined with bicarbonate HCO<sup>3-</sup> and precipitate Calcite, Dolomite and siderite. Figures 7 and 8 show the total amounts of precipitation/dissolution of minerals in the given system. For instance, in the very beginning of the process, the minerals Calcite, Dolomite, Siderite and Kaolinite are represented by negative values of numbers of moles. The dissolution of these four minerals and the other minerals continue until such a point when the dissolutions of the other minerals (e.g., Illite, Annite and Anorthite) begin to provide excess ions (e.g., Ca<sup>++</sup>, Mg<sup>++</sup>, Fe<sup>++</sup>), then the process reverses from the dissolution to precipitation.

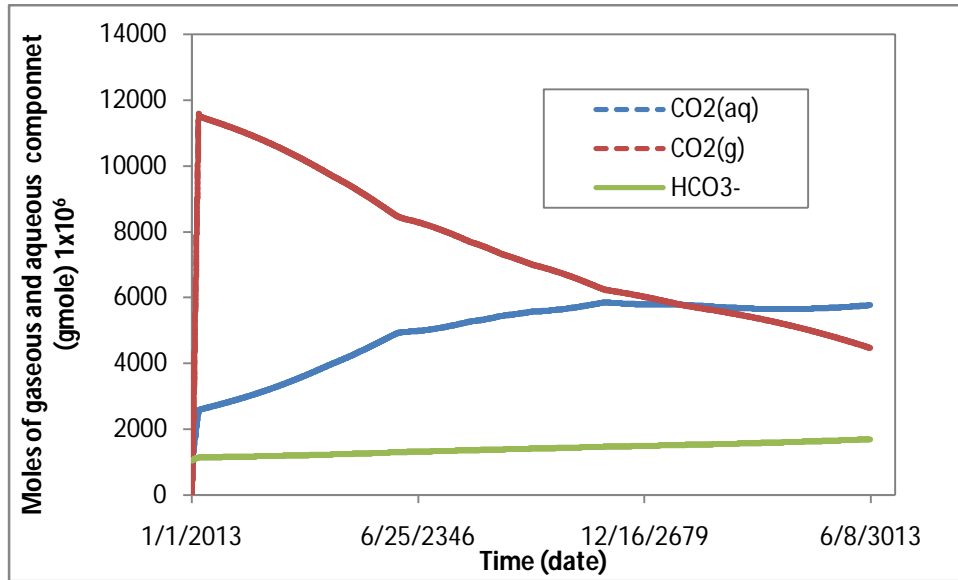


Figure 6: Evolution of CO<sub>2</sub> (g), CO<sub>2</sub> (aq) and HCO<sup>3-</sup> versus Time

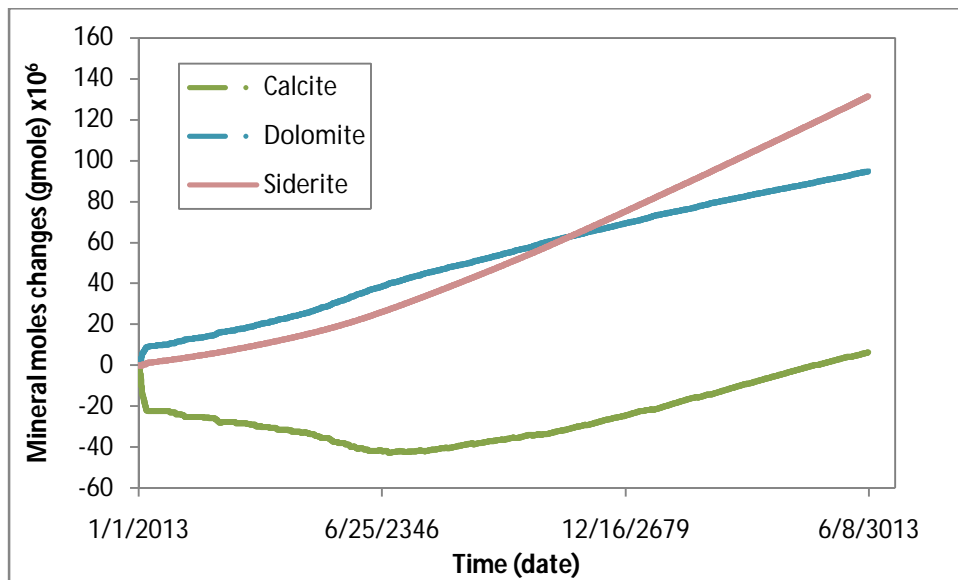


Figure 7: Mineral Precipitation/Dissolution in the System after 100 Years of Simulation

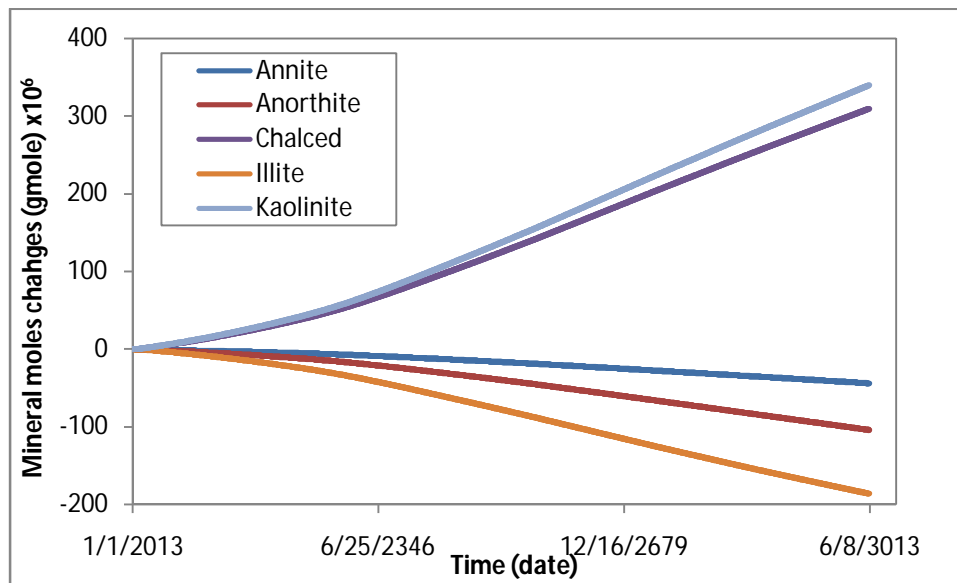


Figure 8: Mineral Precipitation/Dissolution Process after 100 Years Simulation

Table10: Fate of Injected CO<sub>2</sub> under Different Trapping Mechanisms

Trapping Mechanism Types	Residual Trapping through 0.022 S <sub>gr</sub> and Hysteresis		
	Injection phase	Post injection	
		2213 Jan. 01	3013 Jan. 01
Free CO <sub>2</sub> Phase	0.613	0.489	0.247
Total Residual Trapping	0.190	0.240	0.138
Solubility Trapping	0.138	0.196	0.333
Present in Aqueous Ions	0.061	0.062	0.096
Present in Mineral Precipitate	-0.002	0.013	0.186

**Rock property alteration:** Accordingly, rock properties permeability and porosity of the formation are expected to be changed during the dissolution/precipitation processes. Once injection starts, changes in porosity are observed in the areas around the completion wells. Correspondingly, the changes in porosity start to increase vertically, following the trends of upward movement of CO<sub>2</sub> (Figure9). This in turn contributes to mineral dissolution. As stated earlier, the brine saturated with CO<sub>2</sub> would sink due to density differences and as it does so, it reacts with the minerals along the way (Ofori and Engler 2011). Precipitation of the minerals in turn causes the porosity reduction. The reduction in porosity propagates away from the areas around the well in the similar trends of CO<sub>2</sub> convection. Similarly, permeability changes are expected to follow similar trends of porosity (Figures10 and 11). This behaviour is of interest for injectivity enhancement at early stage of injection. In this study, resistance factor is initially predicted by using the Kozeny-Carman relation with adjustable exponent of (c<sub>3</sub>). This exponent of 3 assumes clean formations with relatively smooth shaped grains (Izgec et al. 2008).

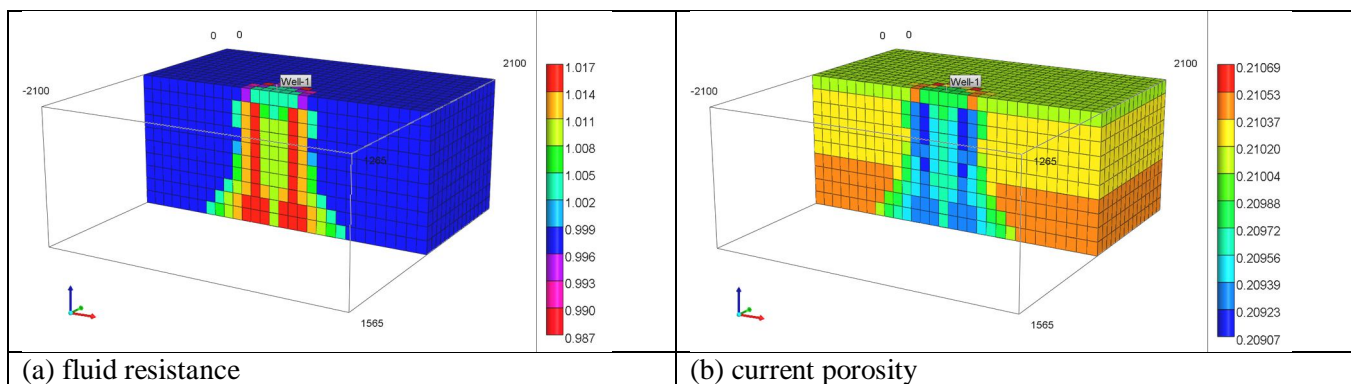


Figure 9: Porosity Distribution Profile and CO<sub>2</sub> Mole Fraction in the Aqueous Phase at Post Injection

According, the phase resistance factor is defined as the ratio between the initial permeability and its current permeability. Since right hand of the equation represent resistance factor of a given phase, permeability changes are controlled through the equation as a function of given porosity.

$$\frac{k}{k_o} = \left(\frac{\phi}{\phi_o}\right)^c \times \left(\frac{(1-\phi_o)}{(1-\phi)}\right)^2 \dots\dots\dots (9)$$

Mineral reactions occurrence effects on host rock properties can be considerable. The simulation results showed changes in porosity, however, the difference is around 0.07% compared to the initial porosity unit. Similarly, the permeability decreased up to 1.2 mD at the end year of the simulation. These results are in agreement with the studies conducted by (Pruess et al. 2003; Xu et al. 2003 and Calabrese et al. 2005).

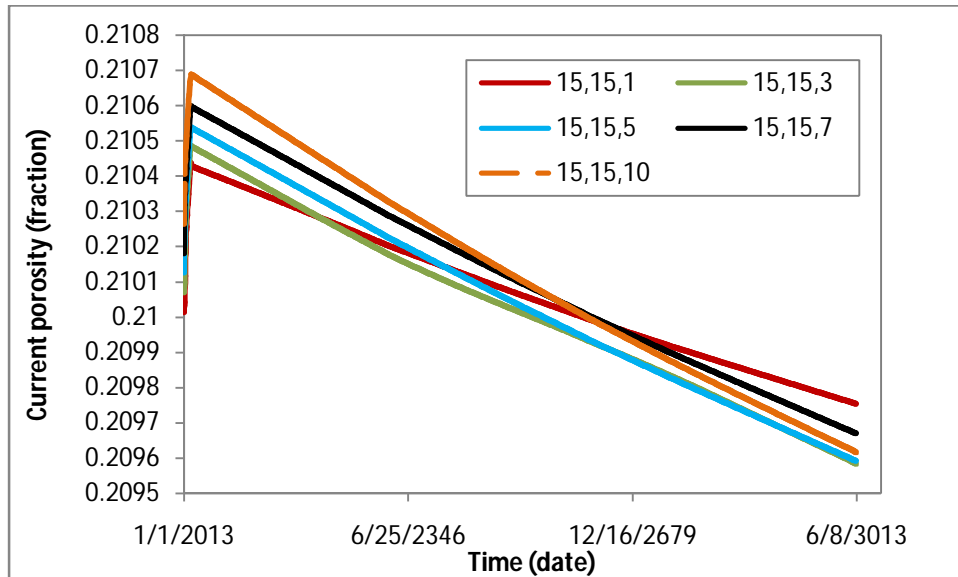


Figure 10: Porosity Changes Profile for Specific Grid-Blocks after 1000 Years of Simulation

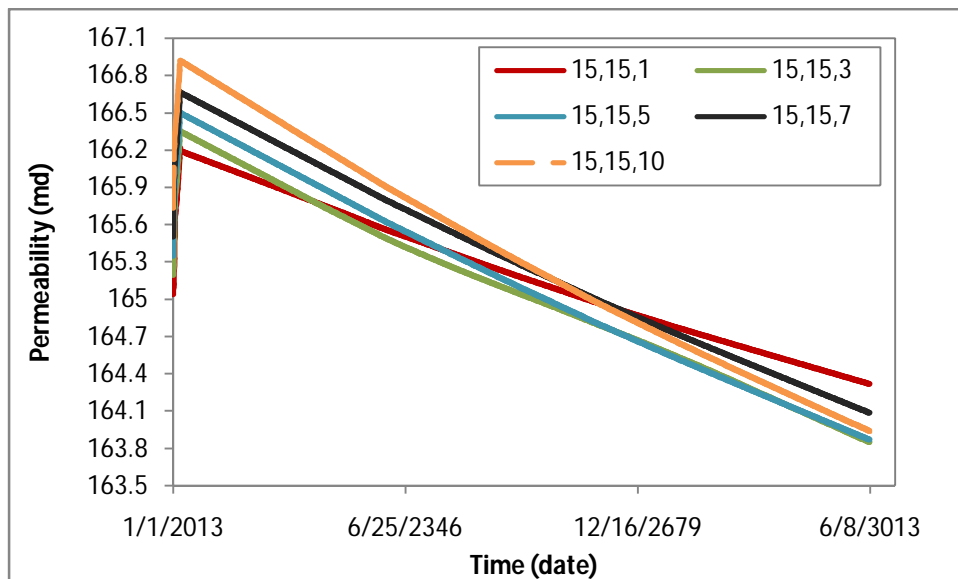


Figure 11: Permeability Changes Profile for Specific Grid-Blocks after 1000 Years of Simulation

#### 4. Summary and Conclusion

Understanding the influence of involved parameters in the process CO<sub>2</sub> storage independently with their contribution on the given trapping mechanisms is helpful to reduce uncertainties associated with the storage and injectivity capacity. Most importantly, this in turn will minimise the risks associated with the leakage through cap rock which possibly can be caused by loss of the integrity of the cap rock due to pressurisation of the formation.

A hypothetical deep saline aquifer is modelled for CO<sub>2</sub> injection using compositional reservoir simulation software GEM-CMG. Fate of injected CO<sub>2</sub> was investigated under different trapping mechanisms for different conditions. Over range of parameters, the study investigated two main tasks. The first task showed the feasibility of CO<sub>2</sub> solubility trapping mechanism on the given aquifers under different reservoir conditions. In geological formations, CO<sub>2</sub> solubility during and after injection process potentially play the most important role in deciding the fate of CO<sub>2</sub> for stabilising and securing the storage mechanisms. The feasibility of solubility trapping mechanism is found to be very case dependent (Table 9). The simulation results showed that aquifers dip and permeability seemed to have a significant effect on CO<sub>2</sub> propagation and dissolution profiles in the formation. In addition, CO<sub>2</sub> storage feasibility under solubility and residual trapping mechanisms were investigated.

The simulation results showed that accounting for hysteresis trapping is essential for predicting CO<sub>2</sub> migration and distribution in the formation when the geological CO<sub>2</sub> sequestration processes are modelled. The second task showed the importance of aquifer mineralogy on the conversion of CO<sub>2</sub> into carbonate minerals in saline aquifer. The processes of dissolution and precipitation are occurred close to the injection well where the gas phase was dominated. In this study, the rate of mineral dissolution and precipitation processes were sufficient enough to change porosity. Mineral precipitation depends highly on the amount and type of the source minerals. Meanwhile, it could lead to enhance geo-chemical reactions with both positive and negative consequences. Changes in the rock properties occurred around the areas surround the well. A small porosity change was resulted in permeability changes by following similar trend of changes. Overall, mineral trapping enhancement is controlled by the solubility trapping. Increase in residual trapping reduces solubility and mineral trapping mechanisms. As it is expected, without considering residual trapping, more CO<sub>2</sub> in the formation will be available to dissolve and lead to increase in HCO<sup>-3</sup> and results in more mineral precipitation. However, more CO<sub>2</sub> is accumulated under the seal. That is, consideration of combined trapping mechanism is essential for CO<sub>2</sub> sequestration modelling since more accurately captures the behaviour of the CO<sub>2</sub> distribution and potentially provides more reasonable insight and support for applications in geological settings especially where structural traps are absent or uncertain.

#### 5. References

- Audigane, P., Gaus, I., Czernichowski, L.I., Pruess, K., Xu, T.: Two-dimensional reactive transport modeling of CO<sub>2</sub> injection in a saline aquifer at the Sleipner site, North Sea. *Am. J. Sci.* 307(7), 974–1008 (2007)
- Bachu, S. (2008). CO<sub>2</sub> storage in geological media: Role, means, status and barriers to deployment. *Progress in Energy and Combustion Science* 34, 254–273
- Bachu, S., and Adams, J. (2003). Sequestration of CO<sub>2</sub> in geological media in response to climate change: capacity of deep saline aquifers to sequester CO<sub>2</sub> in solution. *Energy Conversion and Management* 44 (2003) 3151–3175.
- Bachu, S., Bonijoly, D., Bradshaw, J., Burruss, R., Holloway, S., Christensen, N., and Mathiassen, O. (2007). CO<sub>2</sub> storage capacity estimation: Methodology and gaps. *International Journal of Greenhouse Gas Control*, 1(4), pp 430-443.
- Bachu, S., Gunter, W., and Perkins, E. (1994). Aquifer disposal of CO<sub>2</sub>: Hydrodynamic and mineral trapping. *Energy Conversion and Management* 35(4), pp (269–279)
- Benson, S. (2006). Monitoring Carbon Dioxide Sequestration in Deep Geological Formation for Inventory Verification and Carbon Credits. SPE paper 102833, presented at the SPE Annual Technical Conference and Exhibition held in San Antonio, Texas, U.S.A., 24-27 September.
- Bildstein, O., Kervévan, C., Lagneau, V., Delaplace, P., Crédoz, A., Audigane, P., Perfetti, E., Jacquemet, N., and Jullien, N. (2010). *Oil & Gas Science and Technology*, 65 (23), pp. 485-502.
- Calabrese, M., Masserano, F., Blunt, M. (2005). Simulation of physical-chemical process during carbon dioxide sequestration in geological structures. SPE paper 95820; presented at the 2005 SPE Annual Technical Conference and Exhibition held in Dallas, Texas, USA, 9-12 October 2005.

- CMG-GEM. Advanced Compositional and Unconventional Reservoir Simulator. Version 2012 User's Guide. Computer Modeling Group Ltd., Calgary, Alberta.
- CMG-WinProp. Phase-Behaviour and Fluid Property Program. Version 2012 User's Guide. Computer Modeling Group Ltd., Calgary, Alberta.
- Condor, J., Suebsiri, J., Wilson, M., and Asghari, K.(2010). Carbon Footprint and Principle of Additionality in CO<sub>2</sub>-EOR Projects: The Weyburn Case. SPE paper 138885, presented at the SPE Latin American & Caribbean Petroleum Engineering Conferences held in Lima, Peru, 1-3 December 2010.
- David, L. (1996). Aquifer disposal of carbon dioxide: Hydrodynamic and mineral trapping-Proof of concept. Brian Hitchon (Editor), Geoscience Publishing Ltd. Sherwood Park, Alberta, Canada.
- Doughty, C. (2006). Modelling geologic storage of carbon dioxide: Comparison of non-hysteretic and hysteretic characteristic curves. In PROCEEDINGS, TOUGH Symposium, Lawrence Berkeley National Laboratory, Berkeley, California, May 15–17, 2006.
- Evans, B. (2012). Predicting CO<sub>2</sub> injectivity properties for application at CCS sites. Report number 3-1110-0122. Curtin University, published by Global CCS Institute.
- Flett, M., Gurton, D., Weir, G.(2007). Heterogeneous saline formations for carbon dioxide disposal: Impact of varying heterogeneity on containment and trapping. *Journal of Petroleum Science and Engineering*, 57(2), pp 106-118.
- Ghanbari, S., Al-Zaabi, Y., Pickup, G., Mackay, E., Gozalpour, F., and Todd, A. (2006). Simulation of CO<sub>2</sub> storage in saline aquifer. *Chemical Engineering Research and Design*, 48(9), pp 764-775.
- Gunter, W., Perkins, E., and McCann, T. (1993). Aquifer disposal of CO<sub>2</sub>-rich gases: Reaction design for added capacity. *Energy Conversion and Management*, 34(941-948).
- Hitchon, B., Gunter, W., and Gentzis, T. (1996). The serendipitous association of sedimentary basins and greenhouse gases. *American Chemical Society, Division of Fuel Chemistry*, 41(4), pp 1428-1432.
- Hovorka, S.D., Doughty, C., and Holtz, M. H., 2004, Testing efficiency of storage in the subsurface: Frio Brine Pilot Experiment, in 7th International Conference on Greenhouse Gas Control Technologies, Vancouver, Canada, September 5–9, unpaginated [5 p.]. GCCC Digital Publication Series #04-01.
- Ide, S., Jessen, K., Franklin, M., and Jr, O. (2007). Storage of CO<sub>2</sub> in saline aquifers: Effects of gravity, viscous, and capillary forces on amount and timing of trapping. *International Journal of Greenhouse Gas Control*, 1(4), pp 481-491.
- IPCC. (2005). IPCC Special Report on Carbon Dioxide Capture and Storage. Prepared by Working Group III of the Intergovernmental Panel on Climate Change [Metz, B., O. Davidson, H. C. de Coninck, M. Loos, and L. A. Meyer (eds.)]. Cambridge University Press, Cambridge, United Kingdom and New York, NY, USA, 442 pp.
- Izgec, O., Demiral, B., Bertin, H., and Akin, S. (2008). Numerical simulation of CO<sub>2</sub> disposal by mineral trapping in deep aquifers. *Applied Geochemistry*, 19(6), pp 917–936
- Juanes, R., Spiteri, E., Orr Jr, F., and Blunt, M. (2006). Impact of relative permeability hysteresis on geological CO<sub>2</sub> storage. *Water Resources Research*, 42(12), 1-13
- Kestin, J., Khalifa, E. and Correia, J. (1981). Tables of the Dynamic and Kinematic Viscosity of Aqueous NaCl Solutions in the Temperature Range 20-150°C and Pressure Range 0.1–35 MPa. *Journal of Physical and Chemical Reference Data*, 10 (1) 71-87.
- Kumar, A., Ozah, R., Noh, M., Pope, G.A., Bryant, S., Sephehrnoori, K. and Lake, L.W., 2005, Reservoir simulation of CO<sub>2</sub> storage in deep saline aquifers, *SPE Journal*, 10(3): 336–348.
- Kumar, N., and Bryan, S. (2008). Optimizing injection intervals in vertical and horizontal wells for CO<sub>2</sub> sequestration. SPE paper: 116661; SPE Annual Technical Conference and Exhibition, Denver, Colorado, USA, 21-24 September 2008.
- Law, D., Bachu, S., Gunter, W. (1995). CO<sub>2</sub> disposal into Alberta basin aquifers- PhaseIII: Hydrological and numerical analysis of CO<sub>2</sub>-disposal in deep siliciclastic and carbonate aquifers in the Lake Wabamum area. Alberta Research Council, PO Box 8330, Edmonton, Alberta, Canada, T6H 5X2.
- Li, Y.-K. and Nghiem, L. "Phase Equilibria of Oil, Gas and Water/Brine Mixtures from a Cubic Equation of State and Henry's Law," *Can. J. Chem. Eng.*, Vol. 64, pp. 486-496, June 1986.
- Land, C. (1968). Calculation of imbibition relative permeability for two and three phase flow from rock properties. *Society of Petroleum Engineers Journal*, 8(02), pp 149 – 156.

- Mo, S., and Akervoll, I. (2005). Modeling long-term CO<sub>2</sub> storage in aquifer with a black-oil reservoir simulator. SPE paper 93951; presented at the PE/EPA/DOE Exploration and Production Environmental Conference, Galveston, Texas, 7-9 March 2005.
- Nghiem, L., Sammon, P., Grabenstetter, J., and Ohkuma., H. (2004). Modelling CO<sub>2</sub> storage in Aquifers with a fully-coupled geochemical EOS compositional simulator. SPE paper 89474; presented at the SPE/DOE Symposium on Improved Oil Recovery, Tulsa, Oklahoma, 17-21 April 2004.
- Nghiem, L., Shrivastava, V., and Kohse, B. (2011). Modelling aqueous phase behavior and chemical reactions in compositional simulation. SPE paper 141417; presented at the SPE Reservoir Simulation Symposium held in the Woodlands, Texas, U.S.A., 21-23 February 2011.
- Nghiem, L., Shrivastava, V., Kohse, B., Hassam, M., & Yang, C. (2009, January 1). Simulation of Trapping Processes for CO<sub>2</sub> Storage in Saline Aquifers. Petroleum Society of Canada. doi:10.2118/2009-156
- Nghiem, L., Shrivastava, V., Kohse, B., Hassam, M., & Yang, C. (2010, August 1). Simulation and Optimization of Trapping Processes for CO<sub>2</sub> Storage in Saline Aquifers. Society of Petroleum Engineers. doi:10.2118/139429-PA
- Ofori, A., and Engler, A. Effects of CO<sub>2</sub> sequestration on the petro-physical properties of an aquifer rock. SPE paper 147166; parented at the Canadian Unconventional Resources Conference held in Calgary, Alberta, Canada, 15-17 November 2011.
- Ozah, R., Lakshminarasimhan, S., Pope, G., Sepehrnoori, K., Bryant, S. (2005). Numerical simulation of the storage of pure CO<sub>2</sub> and CO<sub>2</sub>-H<sub>2</sub>S gas mixtures in deep saline aquifers. SPE Paper; presented at the 2005 SPE Annual Technical Conference and Exhibition held in Dallas, Texas, U.S.A., 9 – 12 October 2005.
- Peng, Y., and Robinson, B. (1976). A New Two-Constant Equation of State. *Industrial & Engineering Chemistry Fundamental*, 15(1), pp 59-64.
- Prevost, H., Fuller, R., Altevogt, A., Bruant, R., and Scherer, G. (2005). Numerical Modeling of Carbon Dioxide injection and transport in deep saline aquifers. *Greenhouse Gas Control Technologies*, Volume II, 2189-2193.
- Pruess, K., Xu, T., Apps, J., and Garcia, Julio. (2003). Numerical modeling of aquifer disposal of CO<sub>2</sub>. *SPE Journal*, 8(1), pp 49-60.
- Pruess, K and Xu, T. (2007). Two-dimentional reactive transport modelling of CO<sub>2</sub> injection in a saline aquifer at the Sleipner site North Sea. *American Journal of science*, 307(7) 9744-1008.
- Reid, C., Prausnitz, M., and Sherwood, K. (19977). *The Properties of Gases and Liquids*, 3rd Edition, McGraw-Hill, New York.
- Rowe, M. and Chou, S. (1970). Pressure-Volume-Temperature-Concentration Relation of Aqueous NaCl Solutions, *Journal of Physical and Chemical Reference Data*, 15 (1), 61-66.
- Sifuentes, W., Giddins, M., and Blunt, M. (2009). Modeling CO<sub>2</sub> storage in aquifers: Assessing the key contributors to uncertainty. SPE paper 123582; SPE Offshore Europe Oil and Gas Conference Exhibition held in Aberdeen, UK, , 8-11 September 2009.
- Total, S., and Nghiem, L. (2007). A modelling study of the role of selected minerals in enhancing CO<sub>2</sub> mineralization during CO<sub>2</sub> aquifer storage. SPE paper 109739; presented at SPE Annual Technical Conference and Exhibition, Anaheim, California, U.S.A, 11-14 November 2007.
- Ukaegbu, C., Gundogan, O., Mackay, E., Pickup, G., Todd, A., and Gozalpour, F.(2009). Simulation of CO<sub>2</sub> storage in a heterogeneous aquifer. *Journal of Power and Energy*, 223(3), pp 249-267
- Xu, T., Apps, J., and Pruess, K. (2003). Numerical simulation of CO<sub>2</sub> disposal by mineral trapping in deep aquifers. *Applied Geochemistry* 19 (6) 917–93